Atmospheric rivers as Lagrangian coherent structures

Daniel Garaboa-Paz , Jorge Eiras-Barca and

Vicente Pérez-Muñuzuri

Group of Nonlinear Physics

University of Santiago de Compostela, Spain

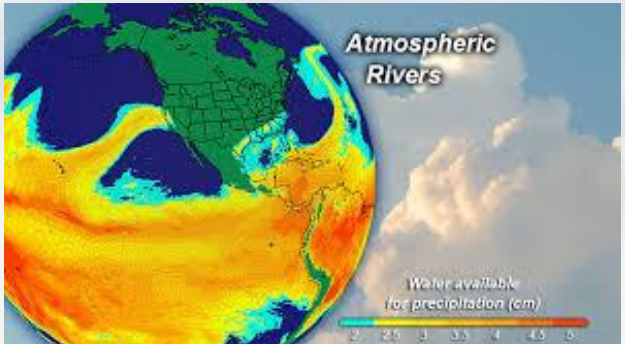

What is an Atmospheric River?

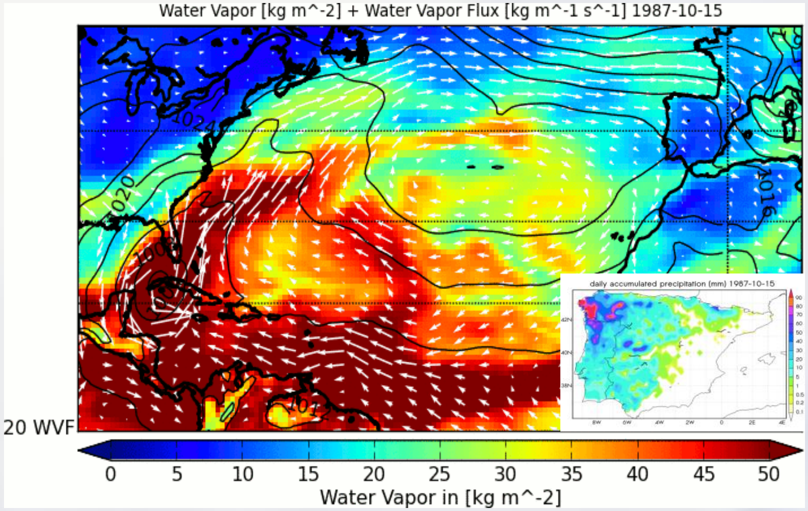
Water Vapor [kg m^-2] + Water Vapor Flux [kg m^-1 s^-1] 1987-10-15

They are narrow structures containing a high amount of water vapor. The largest part of the moisture is located in the first 3 km of the vertical column.

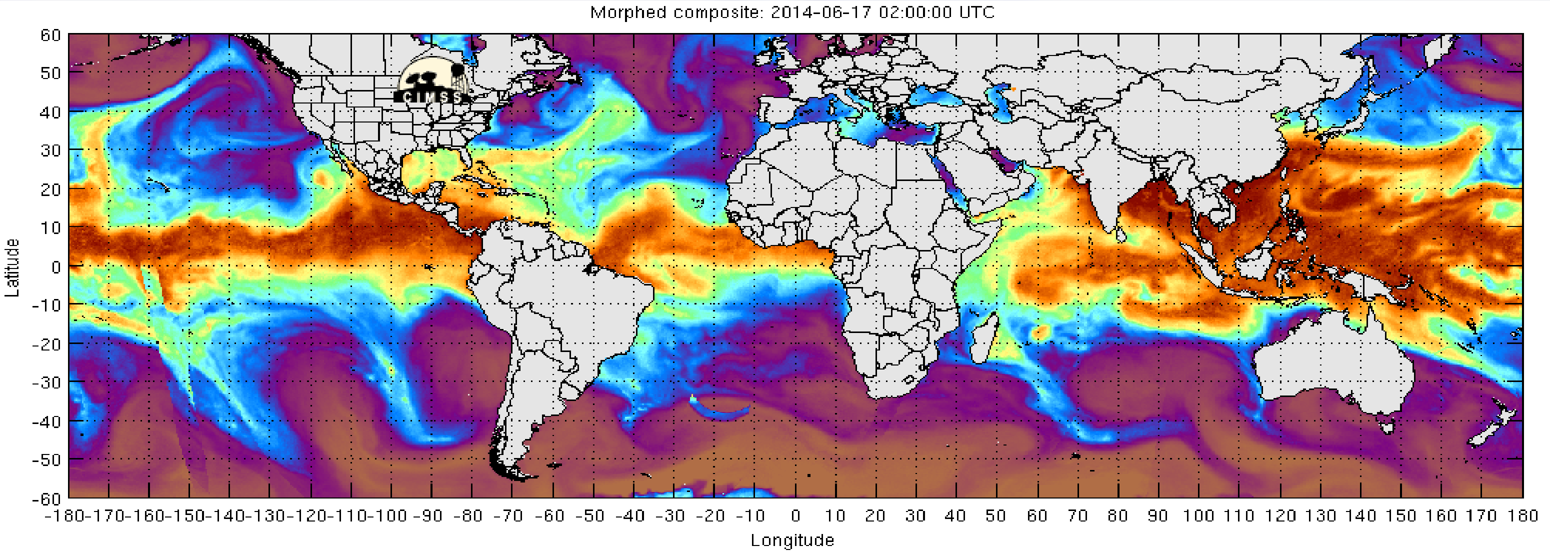
Morphed composite: 2014-06-17 02:00:00 UTC

ARs as a dynamical system

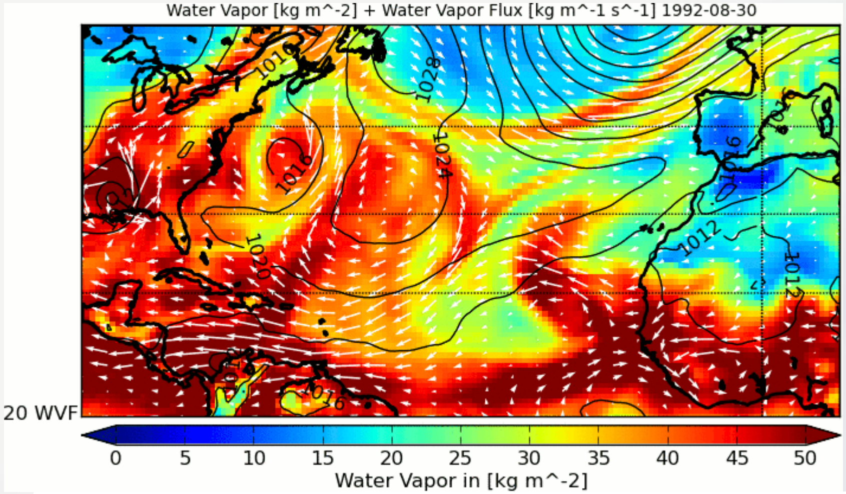
Water Vapor [kg m^-2] + Water Vapor Flux [kg m^-1 s^-1] 1992-08-30

$$Q = \frac{1}{g}\int_0^1 q\frac{\partial p}{\partial \eta}d\eta$$

$$\Phi_\lambda = \frac{1}{g}\int_0^1 uq\frac{\partial p}{\partial \eta}d\eta$$

$$\Phi_\phi = \frac{1}{g}\int_0^1 vq\frac{\partial p}{\partial \eta}d\eta$$

$$\mathbf{V_f} = \left[< \dot{\lambda}(\varphi,\theta,t) >, < \dot{\phi}(\varphi,\theta,t) >\right] = \left[\frac{\Phi_\lambda}{Q}, \frac{\Phi_\phi}{Q}\right].$$

$$\mathbf{V_w} = [u(\varphi,\theta,t), v(\varphi,\theta,t)]_p$$

Q is the vertically integrated water vapor, $\mathbf{\Phi}=(\mathbf{\Phi}_\lambda,\mathbf{\Phi}_\phi)$ is the eastern/northern water vapor flux, *g* is the acceleration of gravity, and η is a hybrid vertical coordinate.

This coordinate uses the mean sea level as a bottom reference level and *p* is the pressure level in the η coordinate.

u and *v* are the eastward and northward wind component and *q* is the specific humidity.

Data from ERA-Interim are available with a spatial resolution of 0.7º and temporal resolution of 6 hours.

2D flow at 850 hPa.

How to extract the flow structure?
Dynamical systems approach to transport

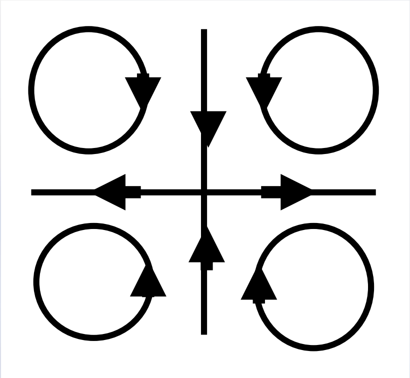

Hyperbolic point and counter-rotating vortices

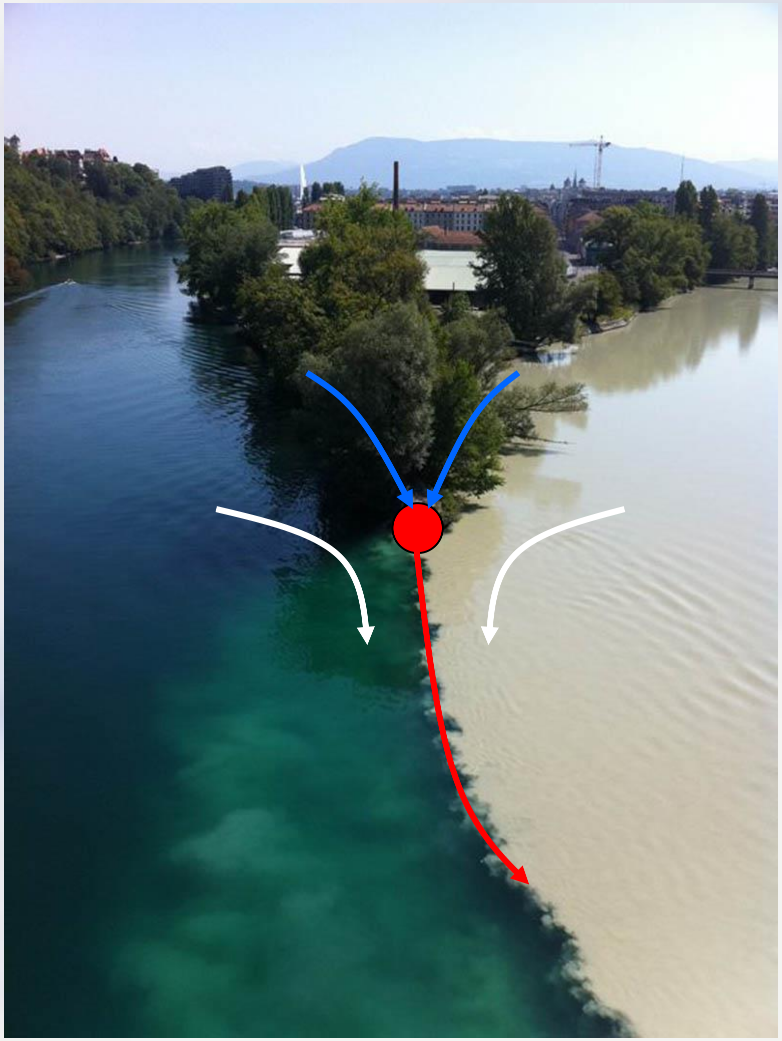

Rhône

Arve

http://twistedsifter.com/2012/04/confluences-around-the-world/

- **Flow as a dynamical system**
- **Hyperbolic point, v=0**
- **Stable and unstable manifolds define a Lagrangian Coherent Structure**

Lagrangian coherent structures
A new view on fluid transport...

- **Coastal currents**

  Shadden et al. (2008), Coulliete et al. (2007), Huhn et al (2014)
- **Studies of bird behavior/ ocean**

  Tew Kai et al.(2009)
- **Ocean circulation, mesoscale eddies**

  BeronVera et al. (2008), d'Ovidio et al. (2004, 2009)
- **Plankton blooms**

  Lehahn et al. (2007)
- **Polar vortex, ozon hole**

  Joseph&Legras (2002), delaCamara et al. (2012)
- **Flow around a jelly fish**

  Dabiri et al. (2009)
- **Flow in blood vessels**

  Arzani&Shadden et al. (2012)

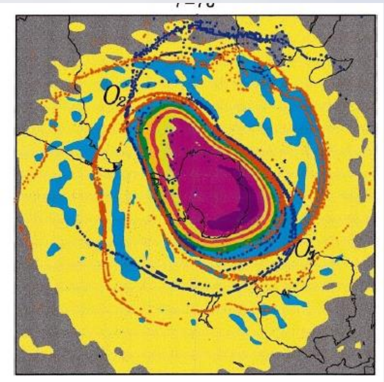

Polar Vortex

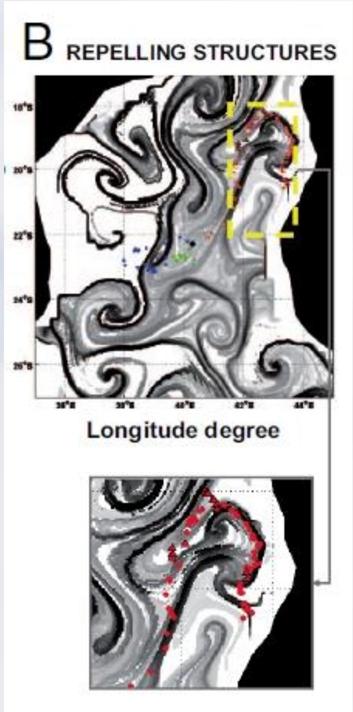

Mozambique Channel

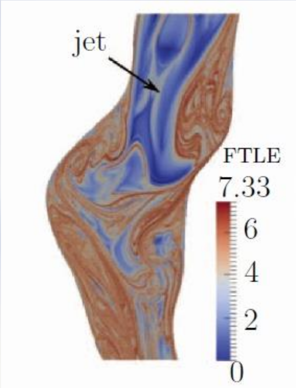

Aortic aneurysm

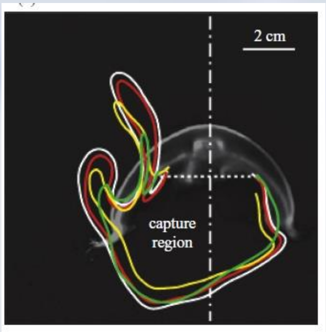

Jellyfish

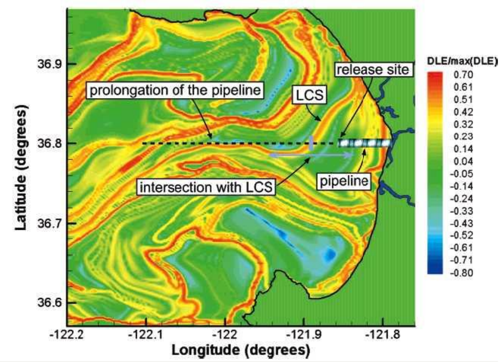

Monterey Bay, Calif.

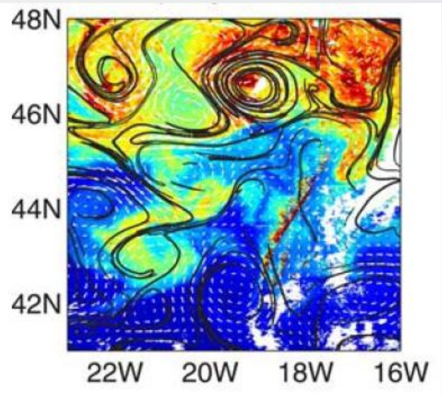

North Atl. Ocean

What is a Lagrangian Coherent Structure (LCS)?

Lagrangian: sit on fluid particle, based on trajectories

coherent: live-time long enough to significantly affect transport

LCS: Definition [Haller (2000, 2011)]

1. Organizing centers for Lagrangian patterns
2. Material lines, hence **transport barriers**
3. LCS exhibit locally the strongest attraction, repulsion or shearing in the flow.

LCS
control the stretching
and folding of the fluid

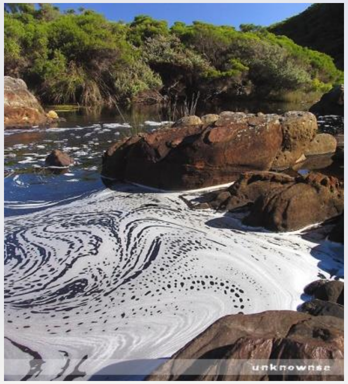

Hyperbolic region

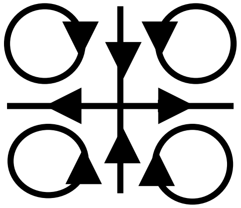

Jet

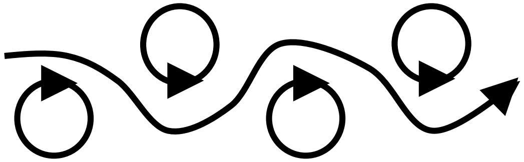

A toy model: Double gyre

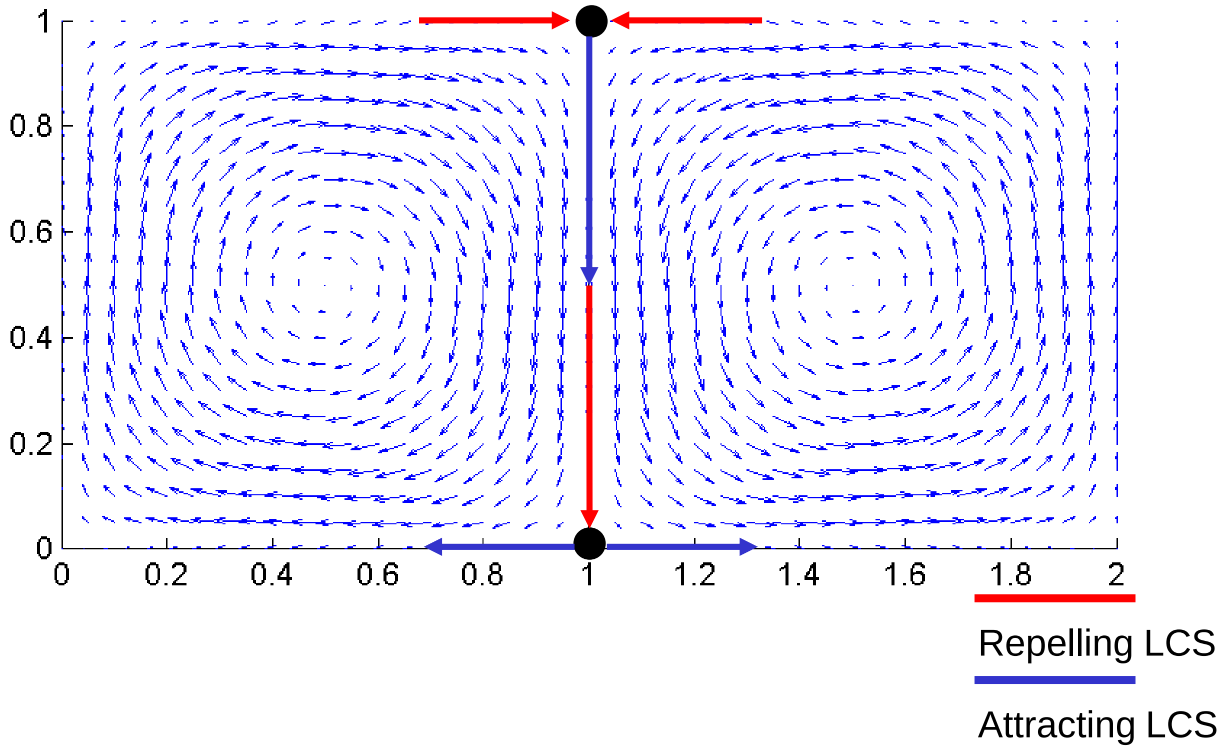

- No mixing!
- Dynamical system, Solutions: Trajectories of fluid parcels
- Phase space = real space (2D)
- Portrait of phase space: hyperbolic fix points, stable and unstable manifolds

$$\dot{\boldsymbol{x}}(t) = \boldsymbol{v}(\boldsymbol{x})$$

A toy model: Double gyre

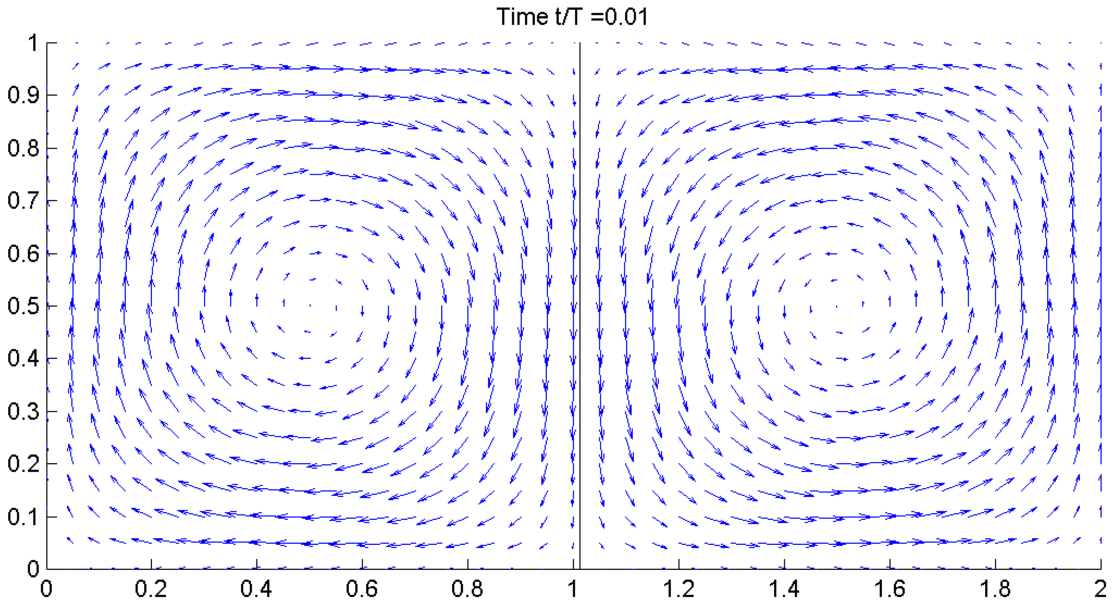

$$\psi(x,y,t) = A\sin(\pi f(x,t))\sin(\pi y)$$

$$\dot{\boldsymbol{x}}(t) = \boldsymbol{v}(\boldsymbol{x}, \boldsymbol{t})$$

$$\begin{aligned} f(x,t) &= a(t)x^2 + b(t)x \\ a(t) &= \epsilon\sin(\omega t) \\ b(t) &= 1 - 2\epsilon\sin(\omega t) \end{aligned}$$

- Mixing? Fluid exchange between eddies?
- Portrait of phase space?
- Simple time-dependent flows can be chaotic

From: Shadden, LCS Tutorial

A toy model: Double gyre

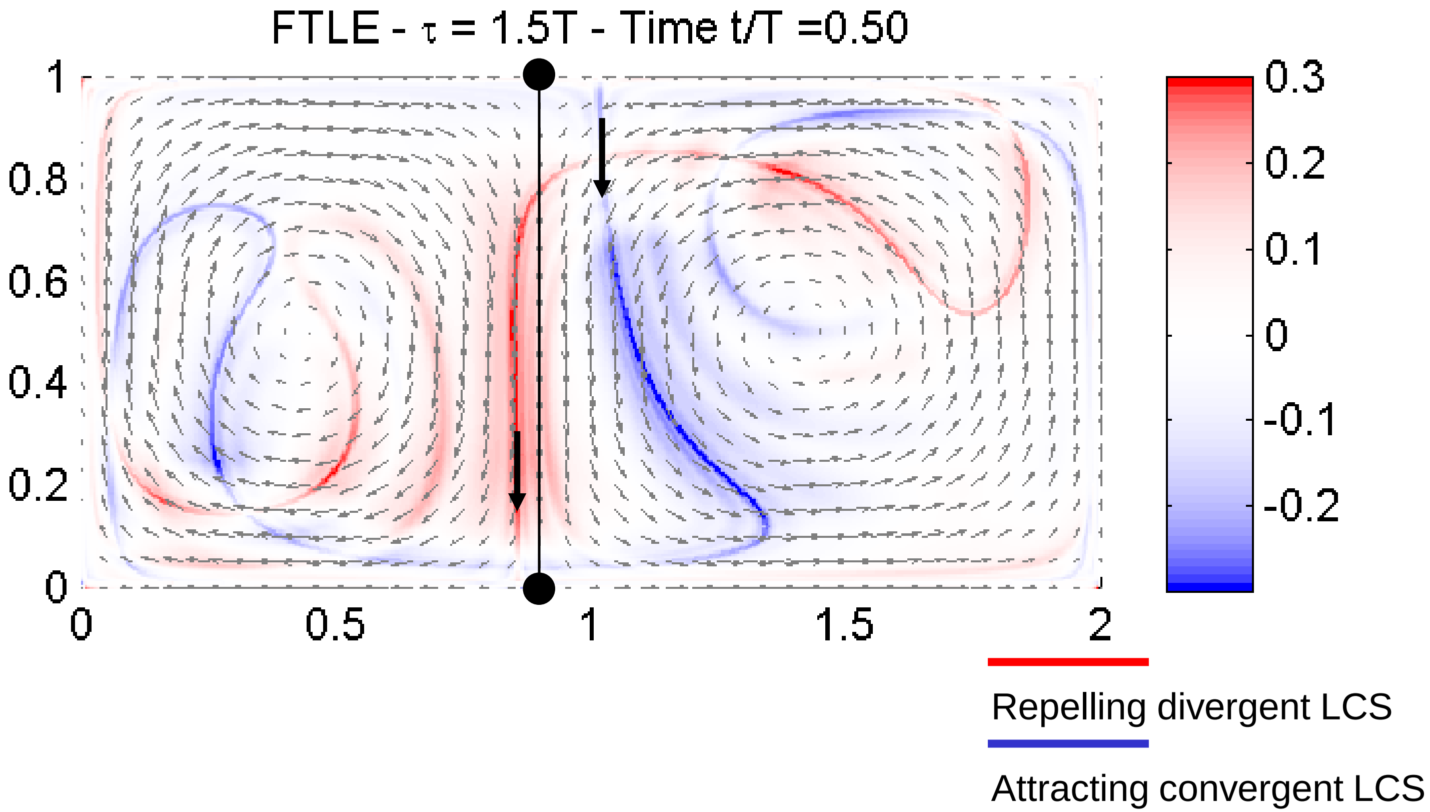

- Heteroclinic tangle – intersecting stable and unstable manifolds of different hyperbolic points
- Fluid in lobes is exchanged between eddies

Finite-Time Lyapunov Exponents (FTLE)

- Lyapunov exponent
- FTLE: Exponential growth rate of infinitesimal perturbations for finite time
- Forward and backward in time (dispersion and convergence)
- Highly dependent on initial position
- **Finite integration time τ**

$$\sigma = \lim_{t\to\infty} \lim_{d_0\to 0} \frac{1}{t} ln\left(\frac{d(t)}{d_0}\right)$$

$$\mathrm{FTLE}\,(t,\tau) \;=\; \frac{1}{\tau}\,\ln\left(\frac{d(t+\tau)}{d(t)}\right)$$

$$\dot{\boldsymbol{x}}(t) = \boldsymbol{v}(\boldsymbol{x},\boldsymbol{t})$$

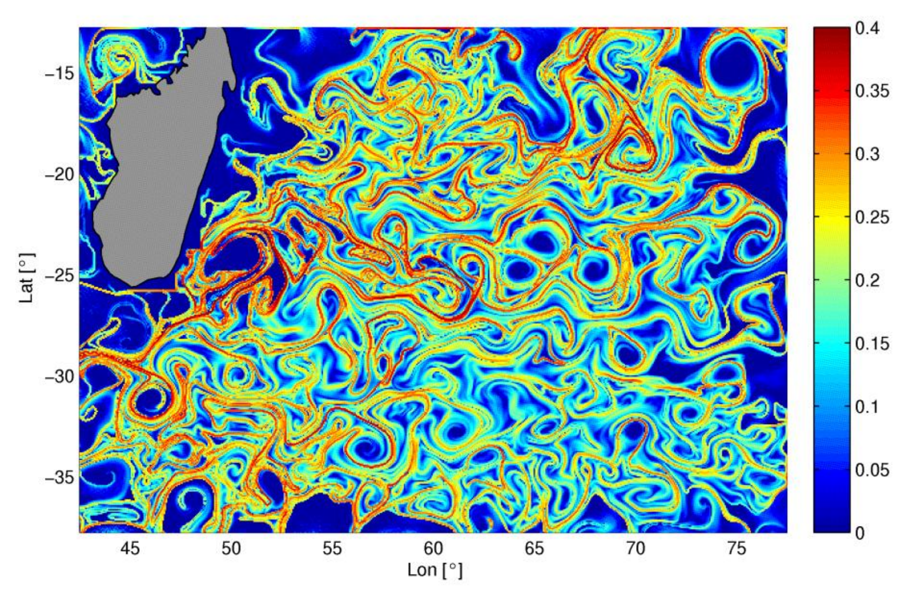

Huhn et al. Geophys. Res. Lett. **39**, L06602 (2012).

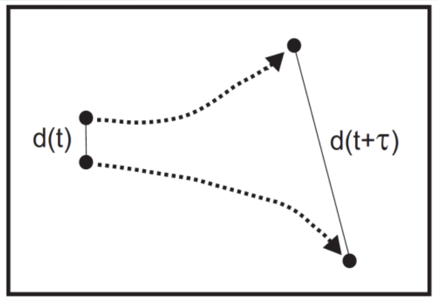

- **Ridges in FTLE field as estimates of hyperbolic manifolds**
- **Approximate material lines**
- **Transport barriers**

Main objective

Given that ARs over the Atlantic and Pacific Ocean appear as coherent filaments of water vapor with a persistence time of several days up to a week, and given that LCSs have turned out to explain the formation of similar tracer patterns in geophysical flows, we address the following questions:

1. **Are ARs associated to attracting LCSs in the large scale tropospheric flow?**
2. **How much do they contribute to the atmospheric mixing?**

FTLE – Computational details

- Flow map $\mathbf{x}(t+\tau) = \varphi_t^{t+\tau}\left(\mathbf{x_0}(t)\right)$

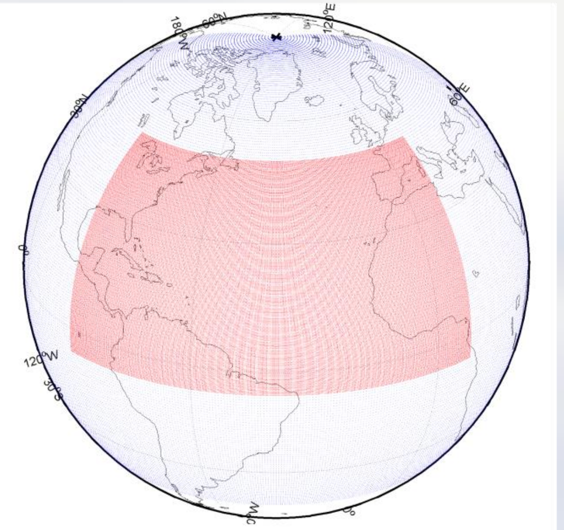

- Finite-time deformation of perturbation

$$\delta\mathbf{x}(t+\tau) \;=\; \nabla\left[\varphi_t^{t+\tau}\left(\mathbf{x_0}(t)\right)\right]\,\delta\mathbf{x_0}(t)$$

- Norm of the deformed perturbation

$$\begin{aligned}\|\delta\mathbf{x}(t+\tau)\| &= \left\langle \delta\mathbf{x_0}(t), \nabla\varphi_t^{t+\tau}(\mathbf{x_0})^T\nabla\varphi_t^{t+\tau}(\mathbf{x_0})\,\delta\mathbf{x_0}(t)\right\rangle^{\frac{1}{2}} \\ &= \left\langle \delta\mathbf{x_0}(t), \mathbf{C}(\mathbf{x_0})\,\delta\mathbf{x_0}(t)\right\rangle^{\frac{1}{2}}\end{aligned}$$

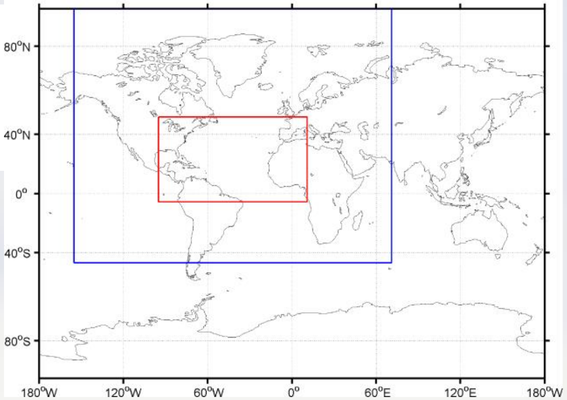

- Finite-time Lyapunov exponent

$$\sigma(\mathbf{r}_0, t_0, \tau) = \frac{1}{|\tau|}\,\log\sqrt{\mu_{max}(\mathbf{C}(\mathbf{r}_0))},$$

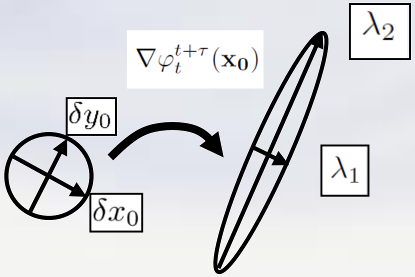

- Simulations in 2D and 3D (from 1000 hPa to 300 hPa)
- Grid of particles with an initial separation of 1/5º
- Multilinear interpolation in time and space
- Integration time is chosen to be τ=120 hours=5 days.
- FTLE calculated backward and forward.

ARs and FTLE

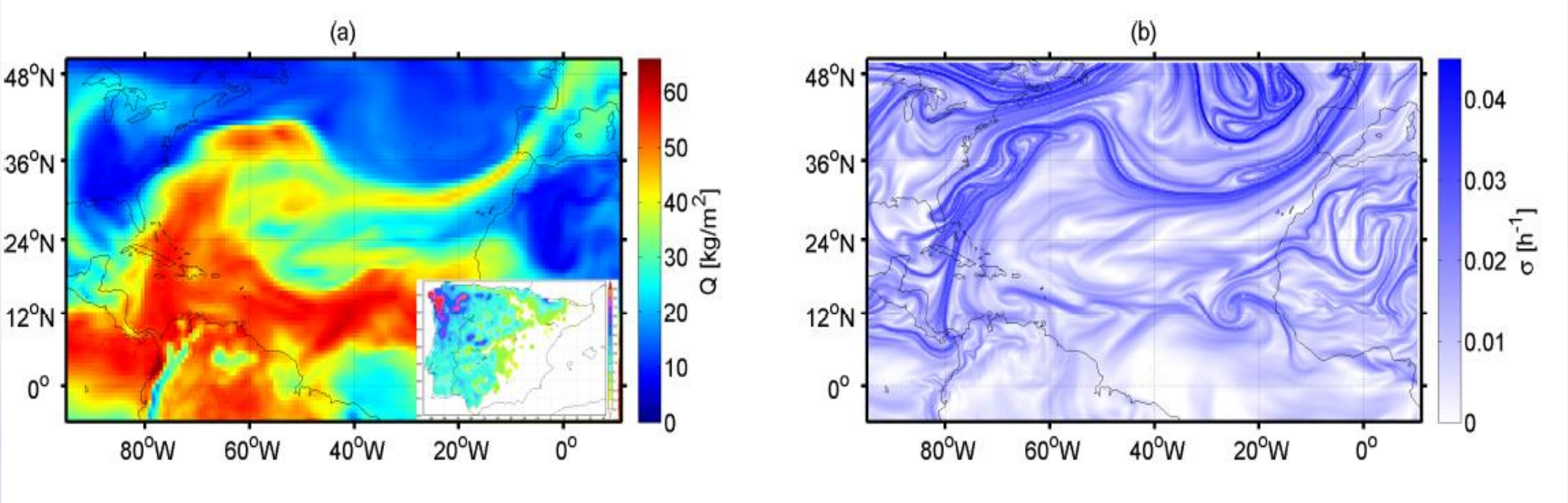

(a) Atmospheric river event on October 15, 1987 in terms of the integrated water vapor column. The inset shows the accumulated precipitation rates over the Iberian Peninsula (mm). (b) Backward FTLE field for the same date and flow.

The ridge represents an attracting LCS of the flow dynamical system. When the AR filament develops, fluid is attracted by the LCS from both sides, and a line of high gradient is generated in the water vapor field.

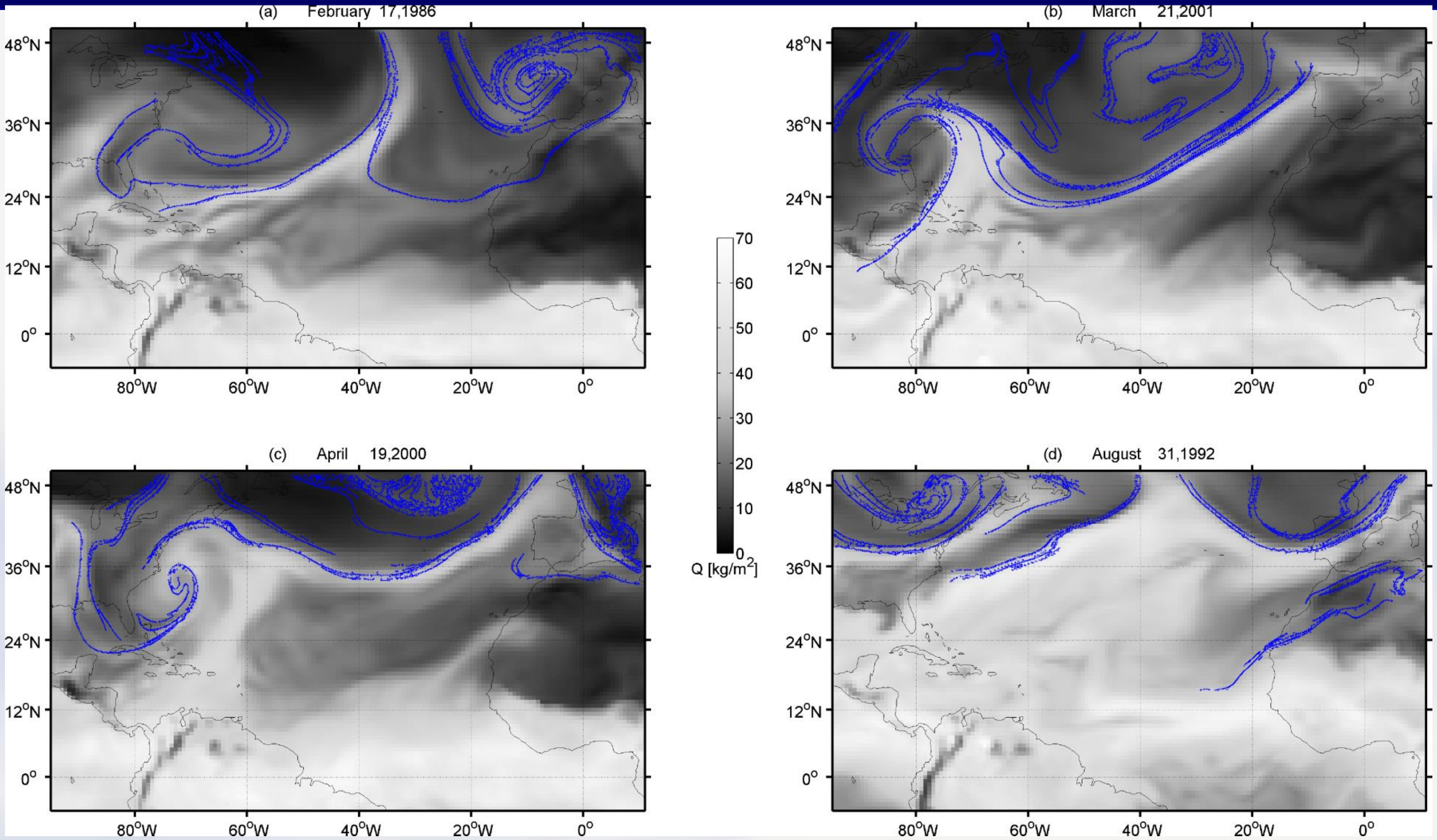

Winter/Spring rivers show more filamentous structures. These filamentous ARs are characterized by one or two narrow filaments growing from low latitudes and transporting water vapor to medium latitudes. In all analyzed winter ARs events, LCSs are located behind the river (in the direction of propagation) and a certain gap in between both ridges, FTLE and Q field, is observed. This suggests that water vapor accumulates in front of the eastwards propagating attracting LCS.

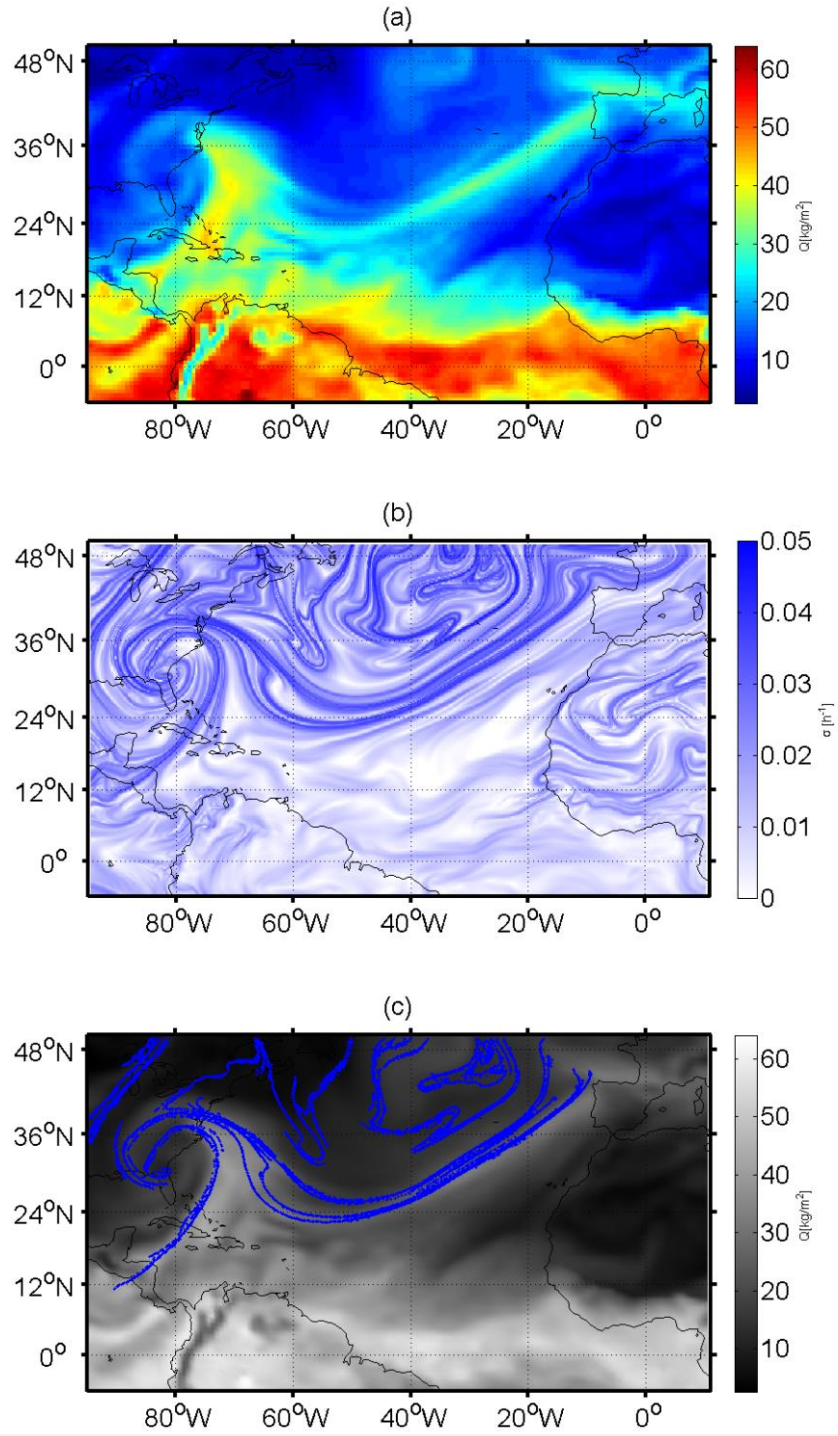
(a)
48°N
36°N
24°N
12°N
0°
80°W
60°W
40°W
20°W
0°
60
50
40
30
20
10
Q[kg/m²]
(b)
0.05
0.04
0.03
0.02
0.01
0
σ [h⁻¹]
(c)
Q[kg/m²]

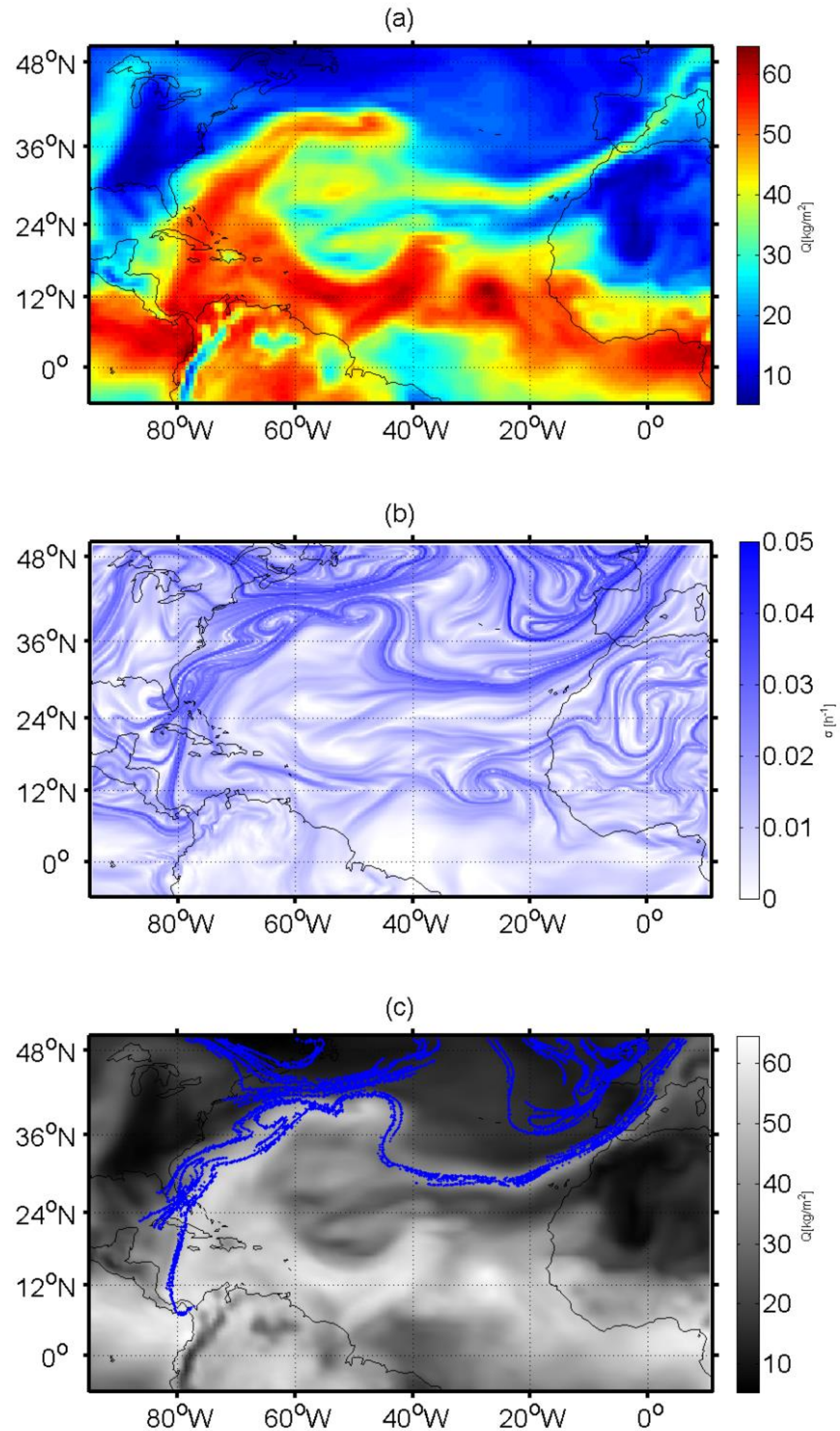
(a)
48°N
36°N
24°N
12°N
0°
80°W
60°W
40°W
20°W
0°
60
50
40
30
20
10
Q[kg/m²]
(b)
0.05
0.04
0.03
0.02
0.01
0
σ [h⁻¹]
(c)
Q[kg/m²]

3D results

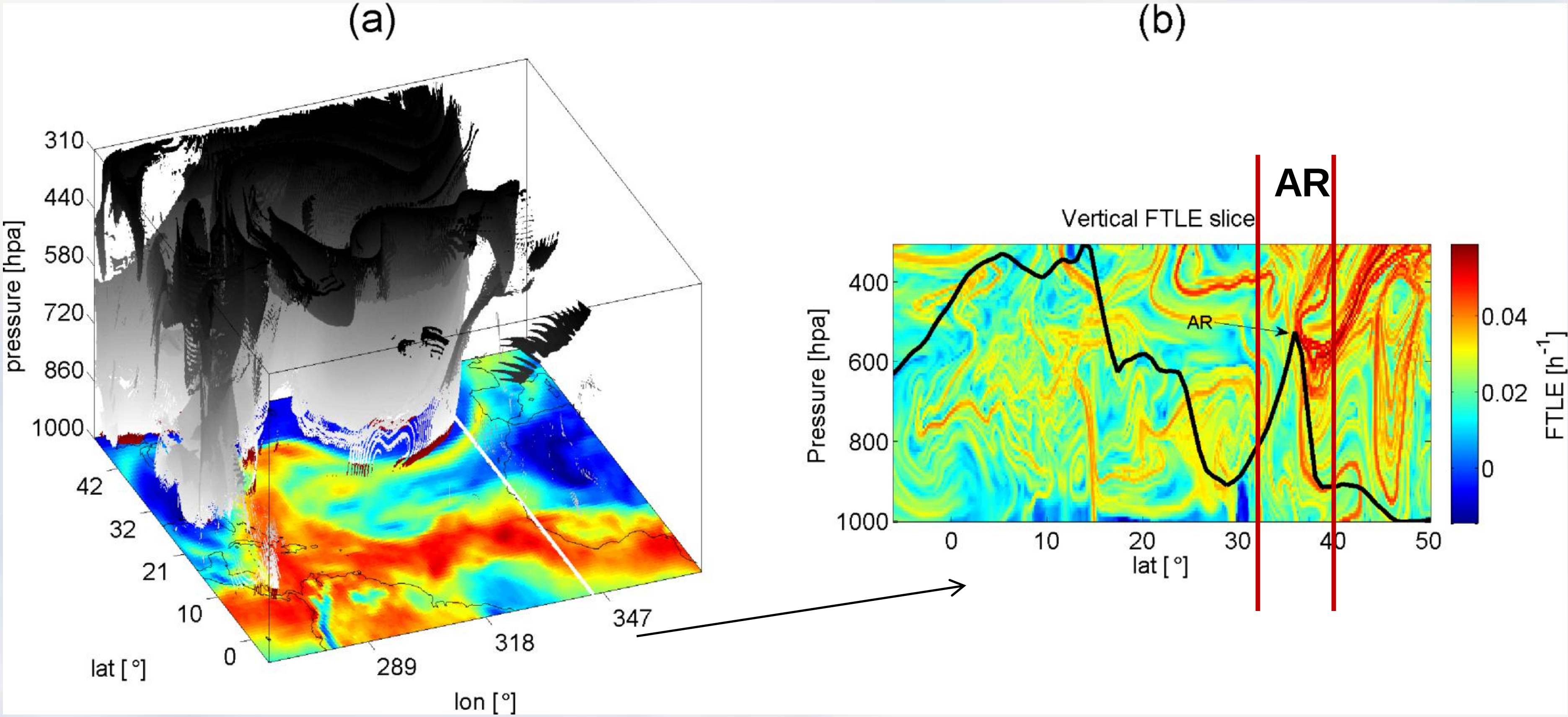

3D LCSs obtained using a fixed isosurface from the FTLE field for a winter AR. Note the ribbon extending from the Tropics towards the Iberian Peninsula. Note the presence of a strong vertically extended FTLE ridge at 35º latitude.

$\phi_z = \rho w (q_v + q_l + q_s),$ **Vertical flux of precipitable water**

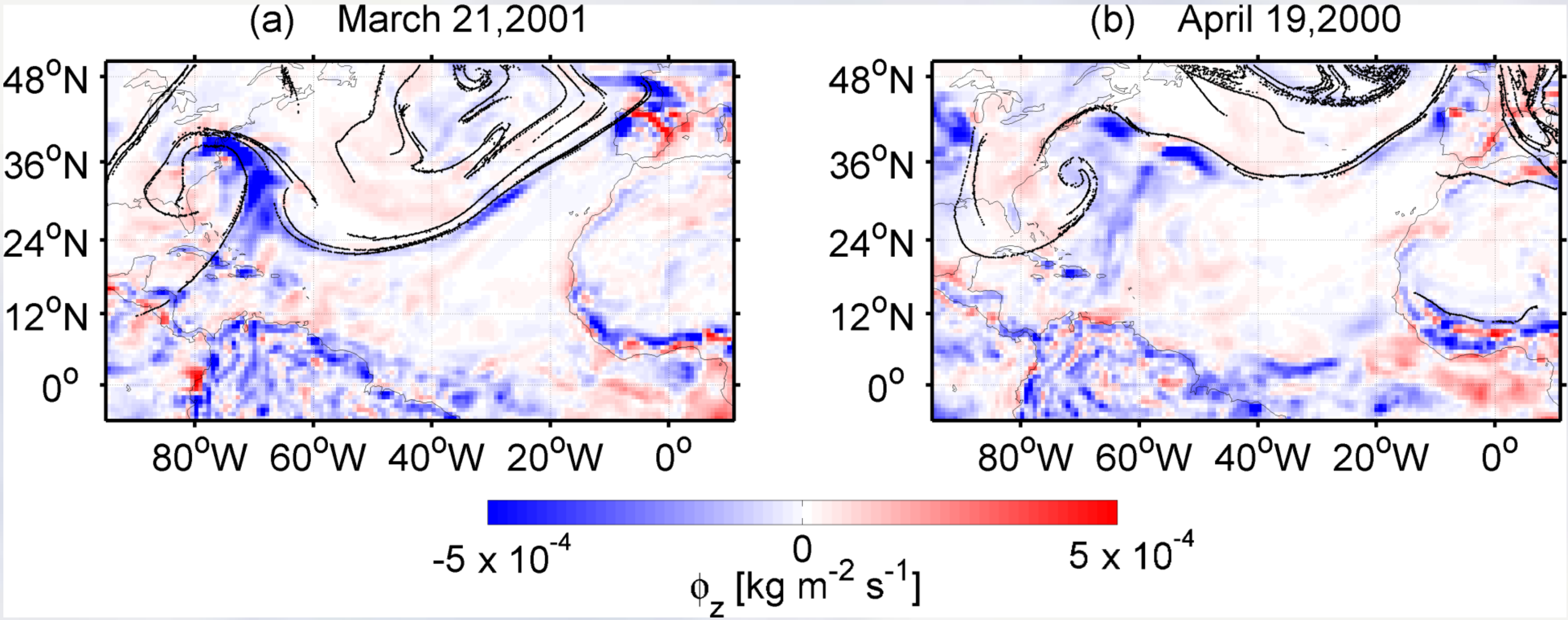

The vertical flux attains maximum values in front of the LCS, but not exactly on top of it. The 3D LCS seems to act as a lateral barrier for the vertical transformation processes of water vapor that develop in front of it as the AR moves eastward, showing that the LCS is a dynamical barrier to precipitable water.

Origin of AR masses

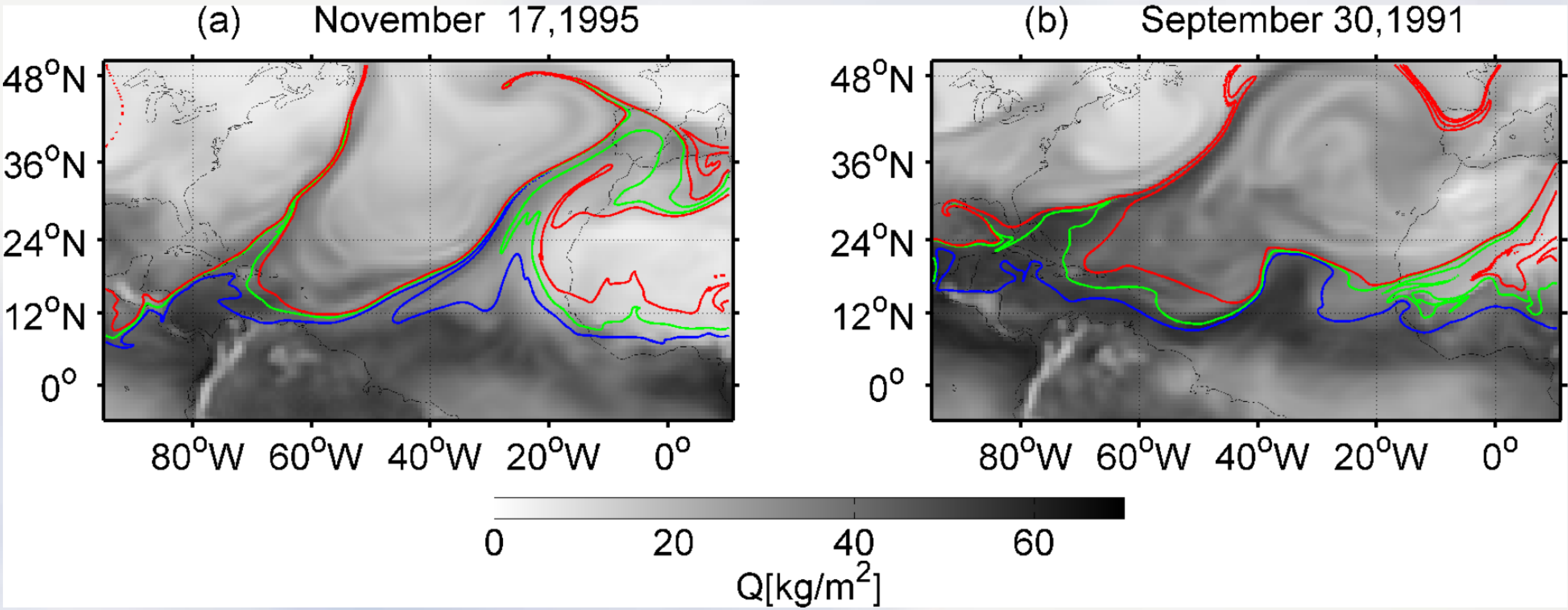

Contours of latitudes of origin of passive tracers advected backward in time for two ARs events. The red, green and blue contours enclose particles coming from 25ºN, 20ºN, and 15ºN. Shaded gray images correspond to water vapor concentration Q.

The percentage of tracers coming from latitudes under 25º is 2.5 times higher than for the September case and 1.5 times higher for latitudes under 20º. Moisture from the Tropics is passively advected northwards, eventually forming the AR. The contribution of evaporation and precipitation can, however, not be assessed with this simple simulation of advection. Both processes tend to represent significant sinks and sources in the water vapor budget.

Questions

1. **Are ARs associated to attracting LCSs in the large scale tropospheric flow?**

YES

[D. Garaboa-Paz and V. Pérez-Muñuzuri, Chaos **25** (2015)]

2. **How much do they contribute to the atmospheric mixing?**

....

FTLE climate time series

The Cauchy-Green tensor should take into account for the spherical coordinates.

$$\dot{\phi} = \omega_1(\phi, \theta, t),$$
$$\dot{\theta} = \omega_2(\phi, \theta, t),$$

From ERA-Interim (1979-2015)

$$\sigma(\mathbf{r}_0, t_0, \tau) = \frac{1}{|\tau|} \log \sqrt{\mu_{max}(\mathbf{C}(\mathbf{r}_0))},$$

$$\bar{C}_{t_0}^{t}(\phi_0, \theta_0) = \begin{pmatrix} \frac{\partial \phi(t; t_0, \phi_0, \theta_0)}{\partial \phi_0} & \frac{\partial \theta(t; t_0, \phi_0, \theta_0)}{\partial \phi_0} \\ \frac{\partial \phi(t; t_0, \phi_0, \theta_0)}{\partial \theta_0} & \frac{\partial \theta(t; t_0, \phi_0, \theta_0)}{\partial \theta_0} \end{pmatrix} \times \begin{pmatrix} r^2 \sin^2 \theta(t; t_0, \phi_0, \theta_0) & 0 \\ 0 & r^2 \end{pmatrix} \times \begin{pmatrix} \frac{\partial \phi(t; t_0, \phi_0, \theta_0)}{\partial \phi_0} & \frac{\partial \phi(t; t_0, \phi_0, \theta_0)}{\partial \theta_0} \\ \frac{\partial \theta(t; t_0, \phi_0, \theta_0)}{\partial \phi_0} & \frac{\partial \theta(t; t_0, \phi_0, \theta_0)}{\partial \theta_0} \end{pmatrix}$$

ERA-INTERIM data:
-Time interval: 1979-2015 with a timestep of 6 hours
-Domain: [0,360]x[-89.5,89.5]
-3D Wind and geopotential data to filter topography.
-Spatial Resolution: 0.7º.
-Temporal Resolution: 6 hours.
-Pressure levels: [900,300] hpa with a resolution of 100 hpa.
-Spatial Resolution: 0.35º
-500000 particles in each advection.
-4-dimensional multilinear interpolation.
-Start a new advection each 6 hours to create the time series.
-Periodic conditions: r(0)=r(360).

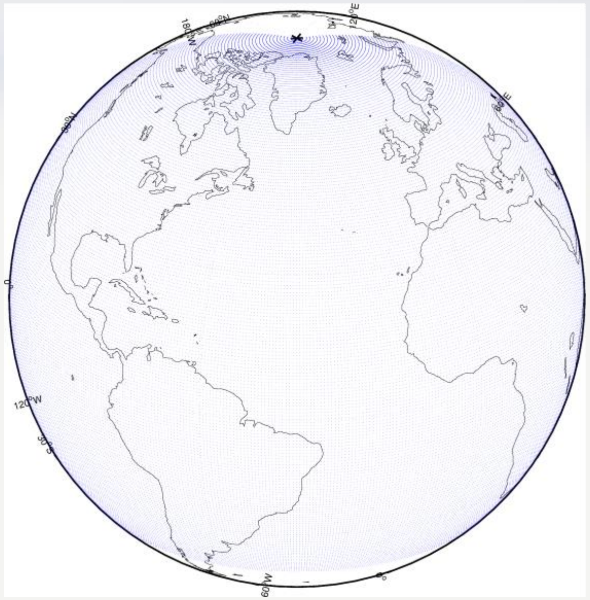

G. Haller and F.J. Beron-Vera, Physica D **241** (2012)

Video

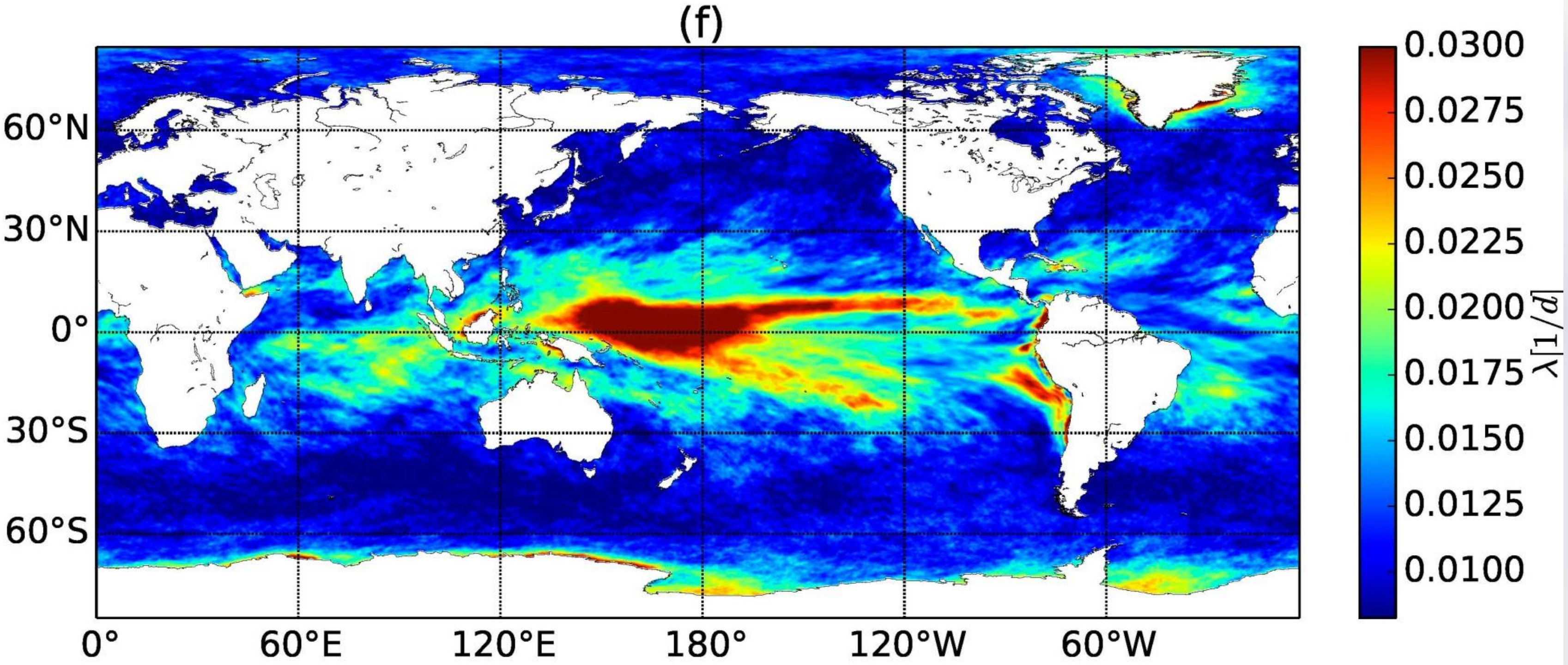

Inter-Annual: Deviation of the mean yearly-data.
ENSO effects are clearly seen. The remainder “periodic” effects are cancelled out.

Backward:
Convergence areas
Forward:
Dispersion areas.

For **backward** propagation, the *Intertropical Convergence Zone (ITCZ)* is emphasized.

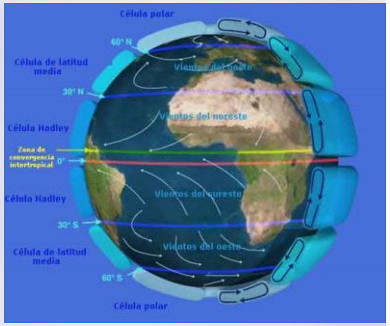

For **forward** propagation, medium latitudes where low and high pressure areas move are emphasized.

Intra-annual

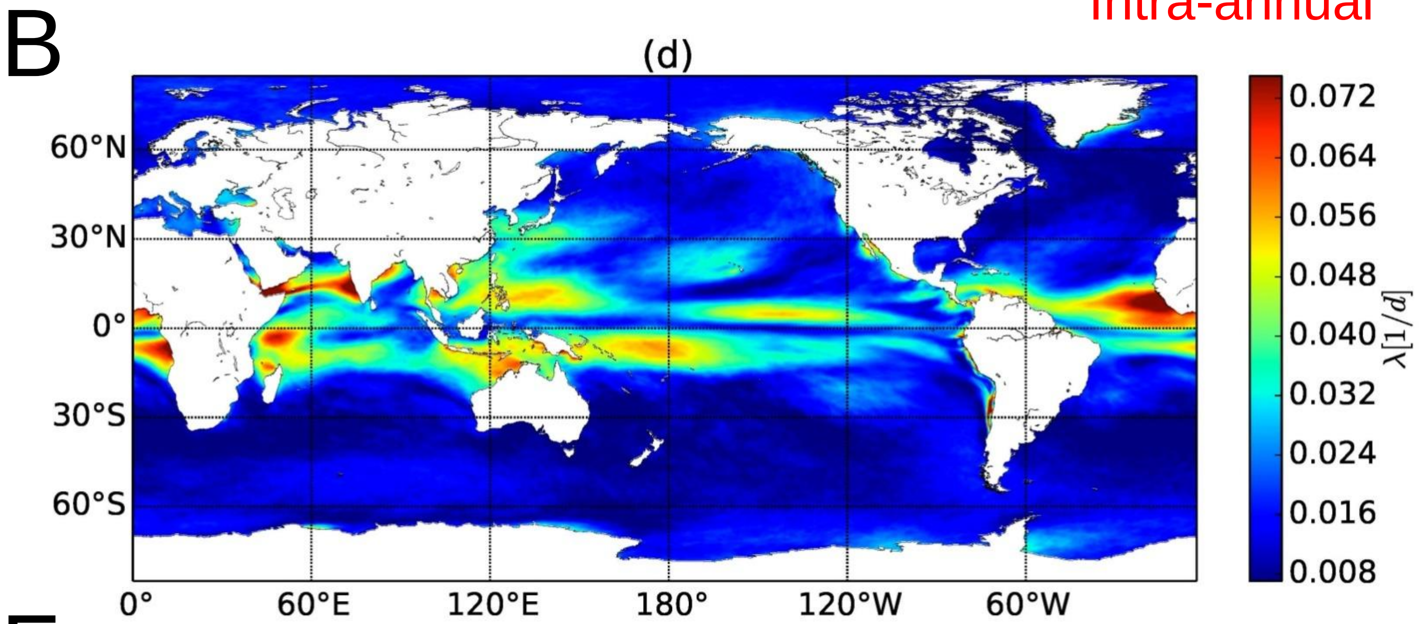

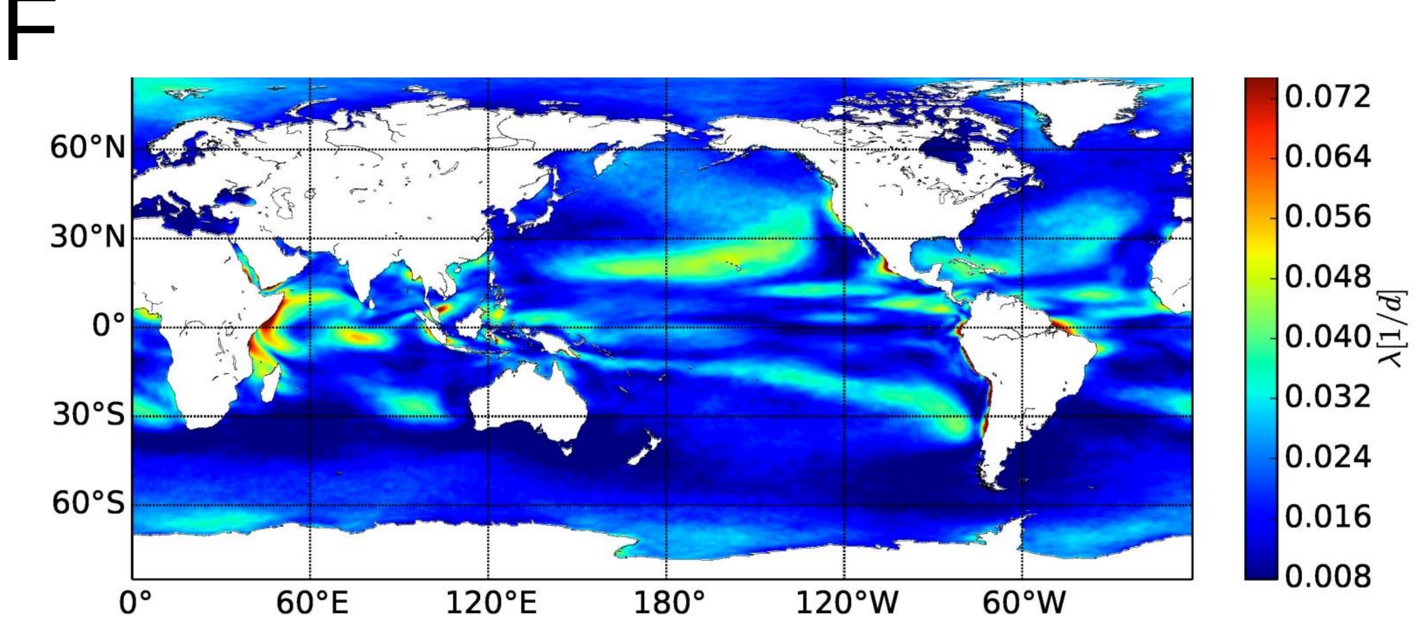

ARs contribution to atmospheric mixing

- An ARs database was created for the 1979-2015 period.
- ARs detection criteria follow from B. Guan and D.E. Wallser, JGR **120** (2015).
- Only landfall events were taken into account.
- FTLE were calculated for timeseries of data with and without AR events.
- We focus on Morocco-Sahara and UK-Ireland regions.

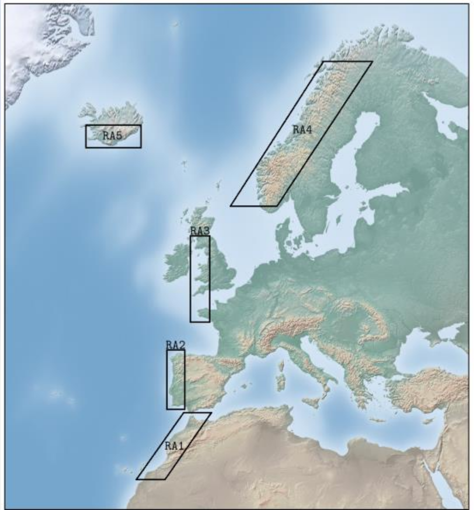

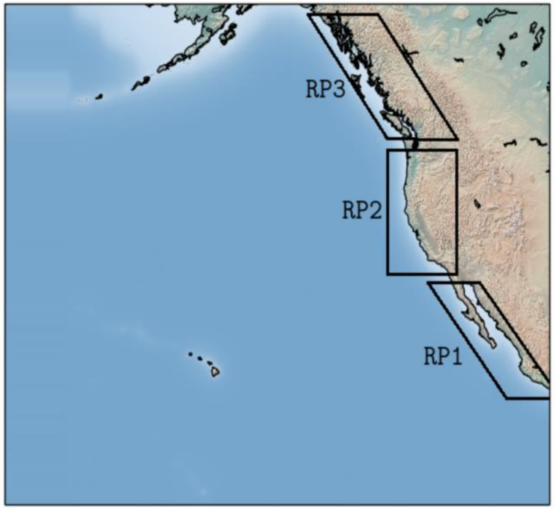

Atmospheric mixing, in terms of FTLE, is 24 larger for Morocco than for UK during AR events, leading to larger precipitation rates. The Morocco-Sahara region has lesser AR activity than UK-Ireland but the contribution to precipitation is more important, in agreement with a larger anomaly in the FTLE backward mixing ratio.

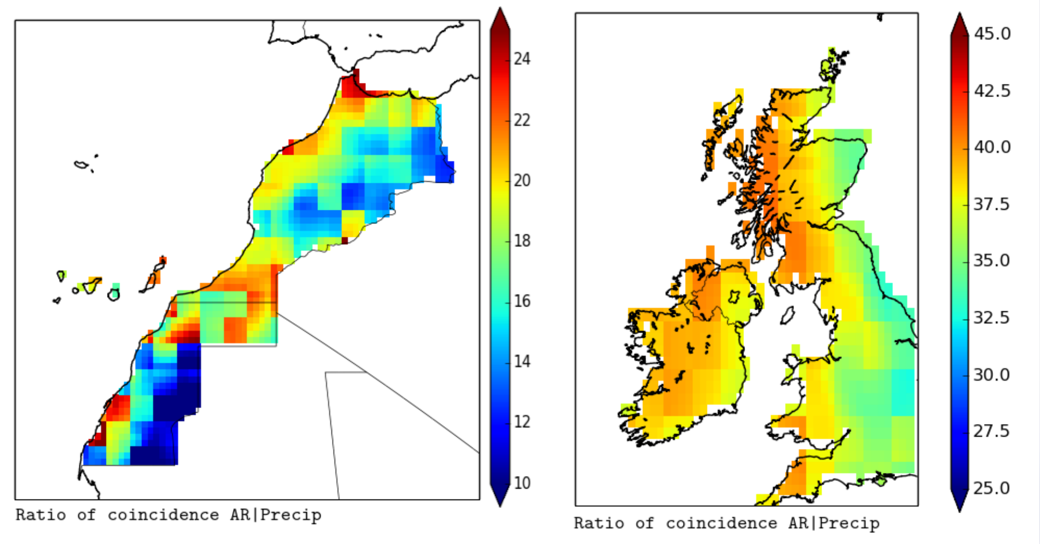

	Morocco-Sahara	UK-Ireland
AR days	10.3% (1201 days)	32.5% (3800 days)
Precipitation	mean: 16.8%, max: 30%	mean: 37.5%, max: 43%
FTLE AR/No-AR	≈ 10-15%	≈ 1-5%

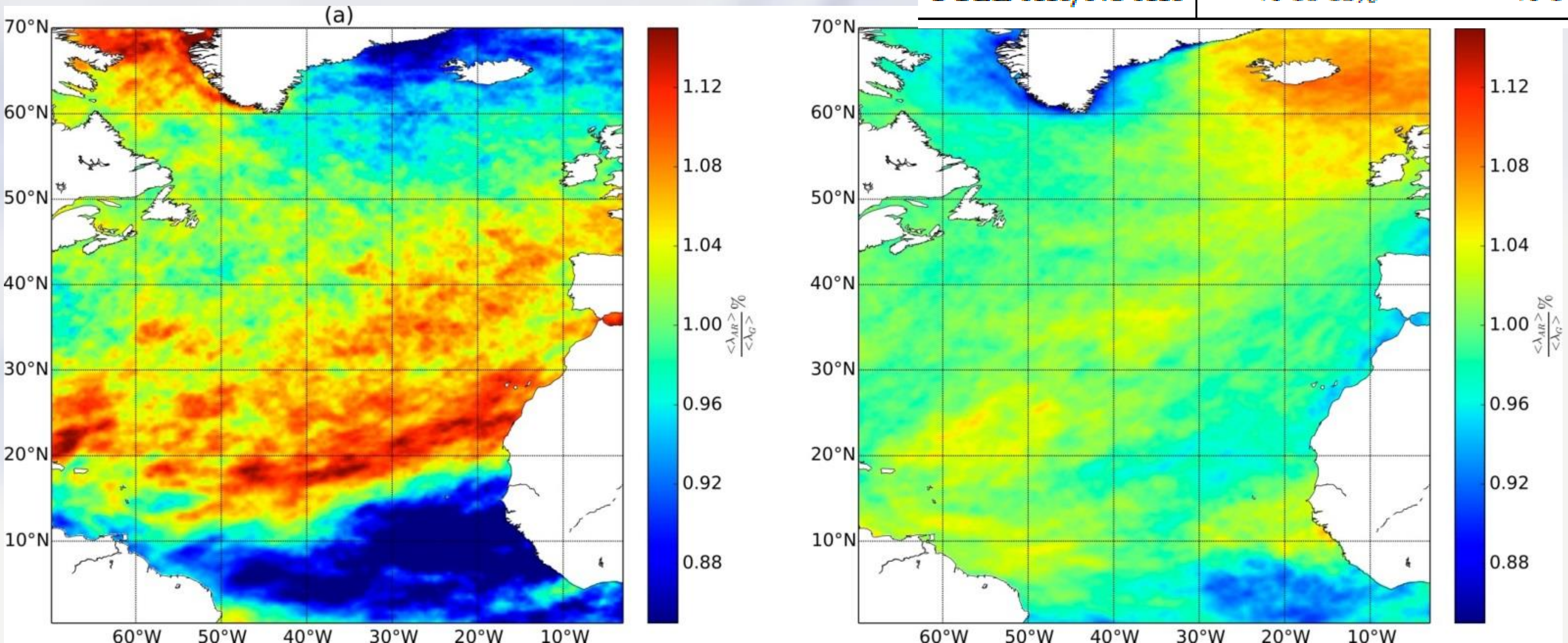

Conclusions

- Narrow filamentous ARs with a fast and persistent eastward transport typically develop in winter. An attracting LCSs with the same shape as the ARs exists in the flow.
- The 2D vertically integrated flow reproduces well the LCSs.
- For non-filamentous rivers, mostly occurring during the summer season, a clear attracting LCS seems to be absent. The water vapor balance of these ARs must be dominated by local sources, since the passive transport of moisture from low latitudes is practically excluded.
- A FTLE climatology has been obtained,
  - Inter and IntraAnnual FTLE maps reproduce well the main circulation patterns.
- The FTLE mean calculated for the AR landfall events points to an increase of mixing near the selected zones. The importance of the ARs in terms of mixing and transport from the Tropics is more important for southern regions than for the northern ones.

Thanks

http://www.usc.es/en/investigacion/grupos/gfnl/

- D. Garaboa-Paz and V. Pérez-Muñuzuri, Chaos **25** (2015)
- Garaboa et al. Submittted GRL (2016).

Using 2D velocity fields

$$\mathbf{V}_\mathbf{w} = [u(\varphi,\theta,t), v(\varphi,\theta,t), w(\varphi,\theta,t)]_p.$$

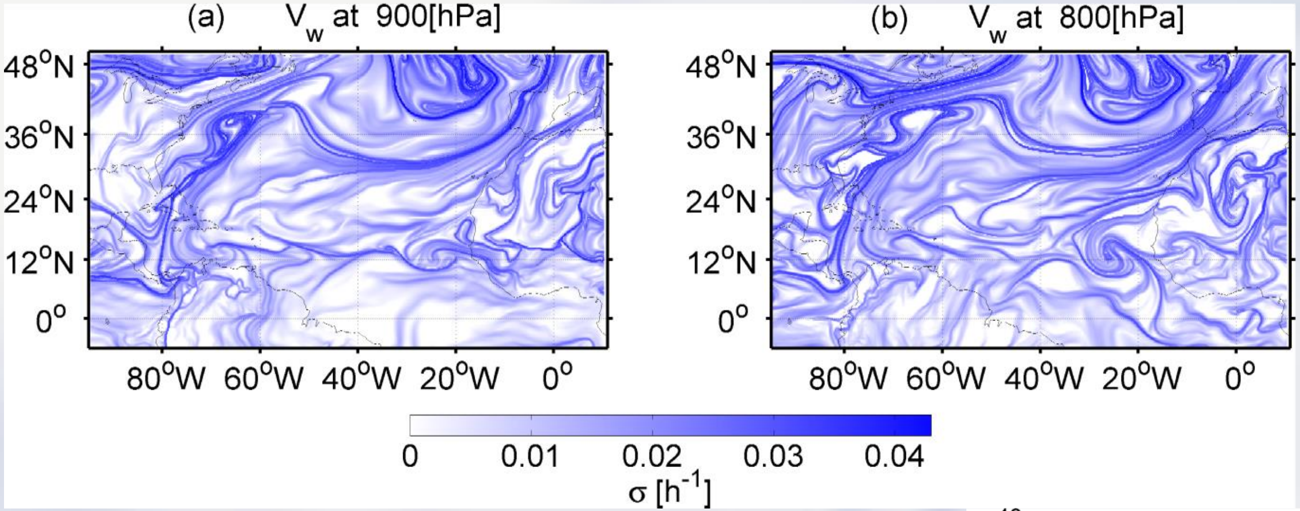

Using V_w instead of the integrated flow V_f gives similar results for pressure leves near 850 hPa.

A minimum of δ is observed for a pressure level near 850 hPa for all ARs events analyzed. The minimum suggests that the flow field at 850 hPa is closest to the water vapor flow V_f.

It is consistent with observations that the core of ARs is typically located at that height [Neiman et al. (2008)].

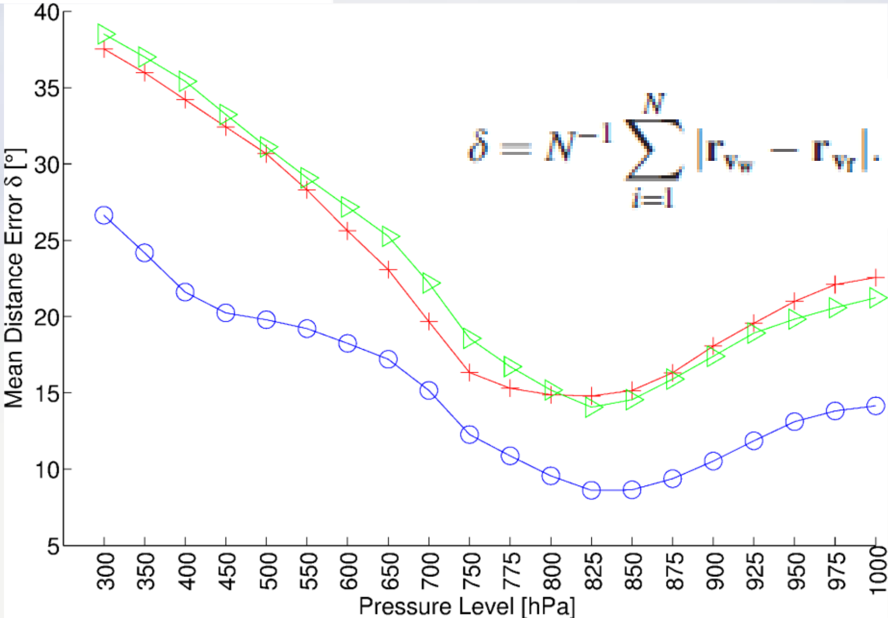

$$\delta = N^{-1}\sum_{i=1}^{N} |\mathbf{r}_{\mathbf{V}_\mathbf{w}} - \mathbf{r}_{\mathbf{V}_\mathbf{f}}|.$$

AR detection criteria

- Thresholding 6-hourly fields of ERA-In IVT (*Integrated Vapor Transport*) based on the 85th percentile.
- Geometry Requirements:
  - Length > 2000 km
  - Length/width ratio > 2
- Coherence Requirements:
  - Coherence in IVT direction : If more than half of the grid cells have IVT deviating more than 45º from the object's mean IVT, the object is discarded.
  - Meridional IVT component > 50 $kg \cdot m^{-1} \cdot s^{-1}$
  - Consistency between object mean IVT direction and overall direction.
- Only landfall events are taken into account.

B. Guan and D.E. Wallser, JGR **120** (2015)